Piquiri fault, Rio Uruguay fault, São Geronimo fault, Rio Alonzo fault and Ferreira fault, and Torres syncline. These cross the long axis of the basin. The Ponta Grossa arch makes the geology of the eastern part of the basin bend toward the interior of the basin. It is more than 600 km in legth and regarded as one of the feeders of the flood basalt lavas. Many dolerite dykes and sills are observed in the direction of NW-SE.

The tectonic direction of E-W is presumed to begin at the same time as the rupture of the Gondwana continent which mean the opening of the Atlantic Ocean in the Cretaceous.

Asuncion Arch runs in the direction of N-S from the eastern part of Paraguay to Mato Grosso do Sul in the western part of the Paraná basin. The arch shows the gentle flexure to the west. The earlier orogenic movement in the western margin of the Gondwana continent is presumed to have involved the Asuncion arch. The Goiania flexure zone in the NW-SE direction is located in the northeastern margin of the Paraná basin. It show strong magnetic anomalies and be accompanied with dykes of alkaline rocks and kimberlites.

1-4-3 Geology and Geological Structure of Basin

The Gondwana continent was undergone successive collisions and tectonic collages during the Brazilian-Pan African orogenic movement and later become a satable continent from the late Pre-Cambrian to the early Paleozoic. The sedimentary rocks are deposited widely from the Paleozoic to Mesozoic in many basins of the Gondwana continent under the extensional stress field. These basins are called intracratonicic basins. The Gondwana continent was ruptured in the Mesozoic. Each segment of continents (South America, Africa, Australia, India, Antarctica) exist several thousand kilometers apart. However, there are many resemblances between the geology of basins on each continent.

The Paraná basin is one of the intracratonic basins which is located in the middle to the south-eastern part of the South American continent. The total area of the basin is 1,400,000 km^2 which consists of 1,100,000 km^2 on the Brazilian side and 300,000 km^2 on the Urguay, Paraguay and Argentine sides. The Paraná basin has an elliptic shape with the sedimentary axis in the NNE-SSW direction. The direction of the axis is in accordance with the direction of the Paraná River. The extension of the basin is 1,750 km from the NNE-SSW direction and 900 km from ESE-WSW direction (Fig. II-1-4-6, Fig. II-1-4-7).

The sediments of the Paraná basin are composed of glacier sediment, desert sandstone and marine sediments. The sediments were formed continuously changing the features as they influenced by several climatic and tectonic changes. The sediments of the basin partccumulated to be more than 6,000 meters thick. Besides, the continental flood basalt which is called the Serra Geral Formation overlie the sediments of the basin. The Serra Geral Formation a large amount of volcanic sequences which is 1,723 meters in maximum thickness.

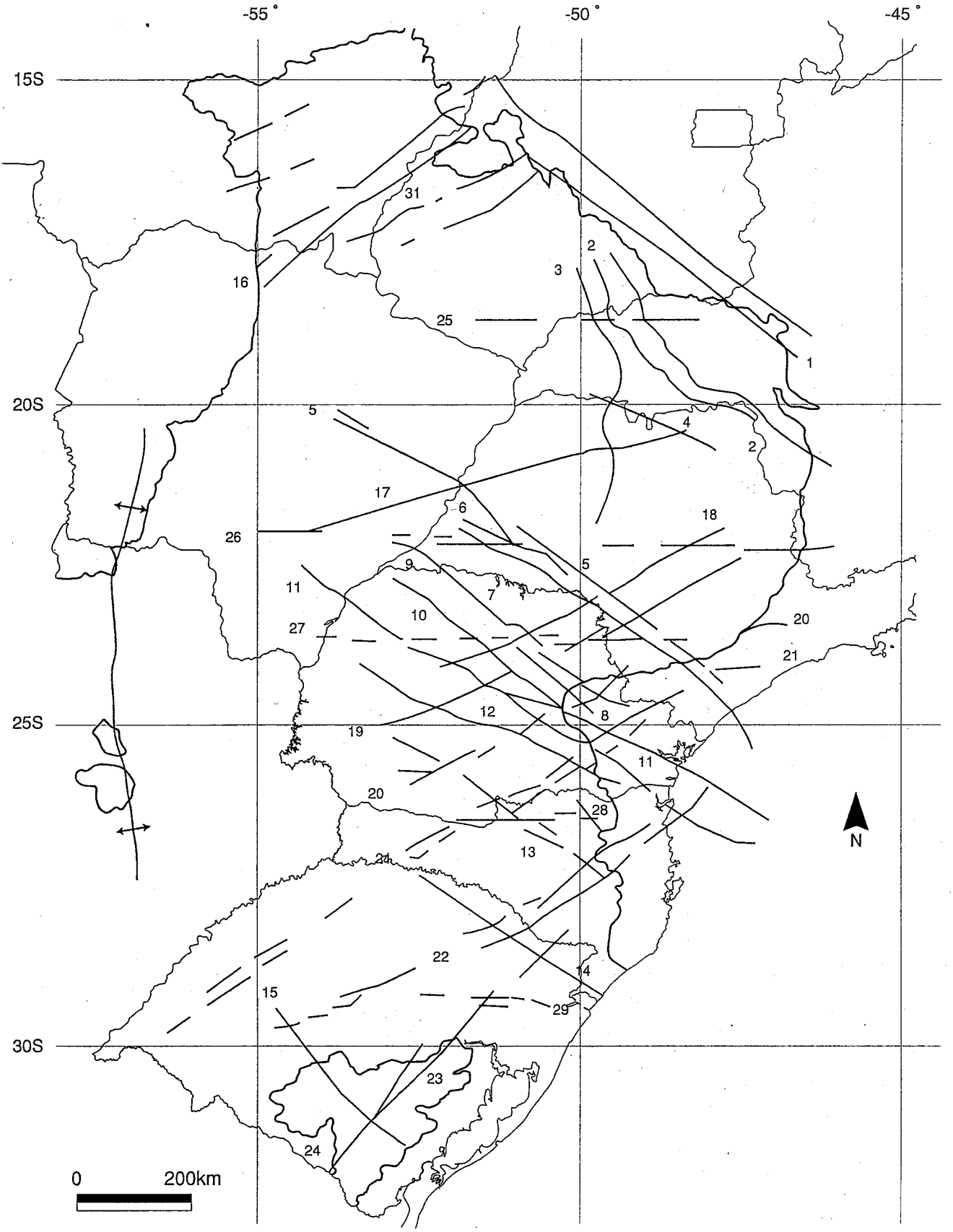

NW-SE direction: ① Arco de Alto Parnaiba; ② Flexura de Goiania; ③ Baixo de Ipiacu/Campina Verde; ④ Alto de Cardoso; ⑤ Zona de Falha de Guapiara; ⑥ Falha de Santo Anastacio; ⑦ Falha de Sao Jeronimo-Curiuva; ⑧ Arco de Ponta Grossa; ⑨ Zona de falha Curitiba-Maringa; ⑩ Falha do Rio Alonzo; ⑪ Zona de Falha Candido de Abreu-Campo Mourao; ⑫ Lineamento do Rio Piquiri; ⑬ Zona de Falha Cacador; ⑭ Sinclinal de Torres; ⑮ Arco do Rio Grande ; ENE-WSW direction: ⑯ Zona de Falha Transbrasiliano; ⑰ Lineamento de Aracatuda; ⑱ Falha de Guaxupe; ⑲ Falha de Jacutinga; ⑳ Zona de Falha de Taxaquara; ㉑ Zona de Falha de Lancinha-Cubatao; ㉒ Zona de Falha Blumenau-Soledade; ㉓ Falha do Leao; ㉔ Falha de Acotea; E-W direction; ㉕ Lineamento Cassilndia; ㉖ Lineamento Moji-Gua-Dourados; ㉗ Lineamento de Sao Sebastiao; ㉘ Lineamento de Taquara Verde; ㉙ Lineamento de Bento Goncalves. N-S direction; ㉚ Arco de Assuncion; ㉛ Domo de Araguainha (Zalan et al.,1988,1990).

Fig. II-1-4-6 Principal archs, faults in the Paraná basin (M.C.L. Quintas, 1995)

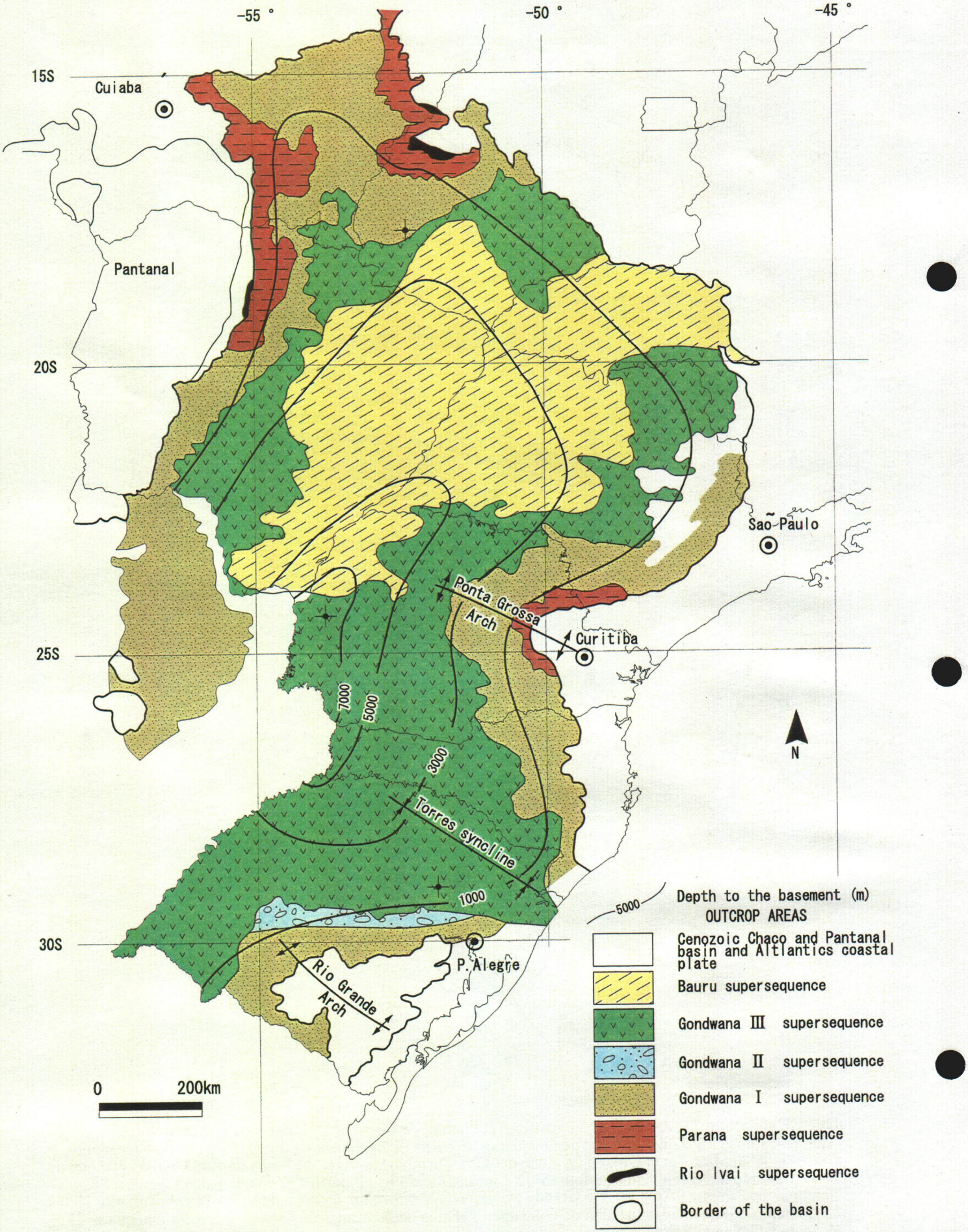

Fig. II-1-4-7 Simplified Geological map of the Paraná basin, with tectonic elements and geographic references (E.J. Milani et al., 1995)

All the sediments of the Paraná basin, from the late Ordovician to the late Cretaceous, can be reviewed by six Supersequence (Fig. II-1-4-8, Milani et al., 1997).

The geology of the Paraná basin can be compared with the world wide transgression and regression (period 390 Ma). The Rio Ivai Supersequence was deposited as the basal sediments of the basin in the Ordovician to the Silurian. In the Devonian, the Paraná Supersequence was deposited by two time transgressions. The Paraná basin was located in the south-east marginal part of the Gondwana continent and was a big bay opening toward the paleo-Pacific Ocean. In the early Carboniferous, the Hercynian orogenic movement occurred and the sediments of the basin were eroded for a long time and became a peneplain. In the late Carboniferous to the Triassic, the Gondwana I and the Gondwana II Supersequences including glacial sediments were widely deposited for a long time. In the Triassic to the Jurassic, the Paraná basin was completely isolated from the ocean, and became the big and dry Gondwana continent. In the early Cretaceous, a large volume of tholeiitic flood basalt magma which is the Gondwana III Supersequence flowed out and the rupture of the Gondwana continent began successively.

Rio Ivai : Ordovician-Silurian (450-428 Ma)
Paraná : Devonian (410-365 Ma)
Godwana I (GI): late Carboniferous-early Triassic (310-245 Ma)
Gondwana II (GII): middle Triassic (237-218 Ma)
Gondwana III (GIII): late Jurassic-middle Cretaceous (150-128 Ma)
Bauru: late Cretaceous (115-65 Ma)

(1) Rio Ivai Supersequence

The oldest sediment of the Paraná basin is the Rio Ivai Supersequence deposited in the late Ordovician to the early Silurian (Fig. II-1-4-9). The Rio Ivai Supersequence overlie on the initial unconformity of the Phanerozoic, which is composed of basal conglomeratio, arkose sandstone, quautzite (Alto Garcas Formation), diamictite (Lapo Formation) and marine shale including fossils (Vila Maria Formation). Vila Maria Formation was deposited in the maximun flooding surface (MFS). The Rio Ivai Supersequence was eroded later and became discontinuous and thinner.

The Rio Ivai Supersequence is several meters to 362 meters thick in Brazil. It becomes thicker toward the west to reach more than 1,100 meters in Paraguay. Still farther west, in Bolivia, the sedimentary rocks which correspond to the Rio Ivai Supersequence were deposited on the marine rift, have the thickness of several thousand meters. The Asuncion arch had never formed in this period. The Rio Ivai Supersequence is considered to have been deposited in the complete open bay of the south-western margin of the Gondwana continent. The subsidence velocity of the basin is considered to be faster due to a strong extensional stress field.

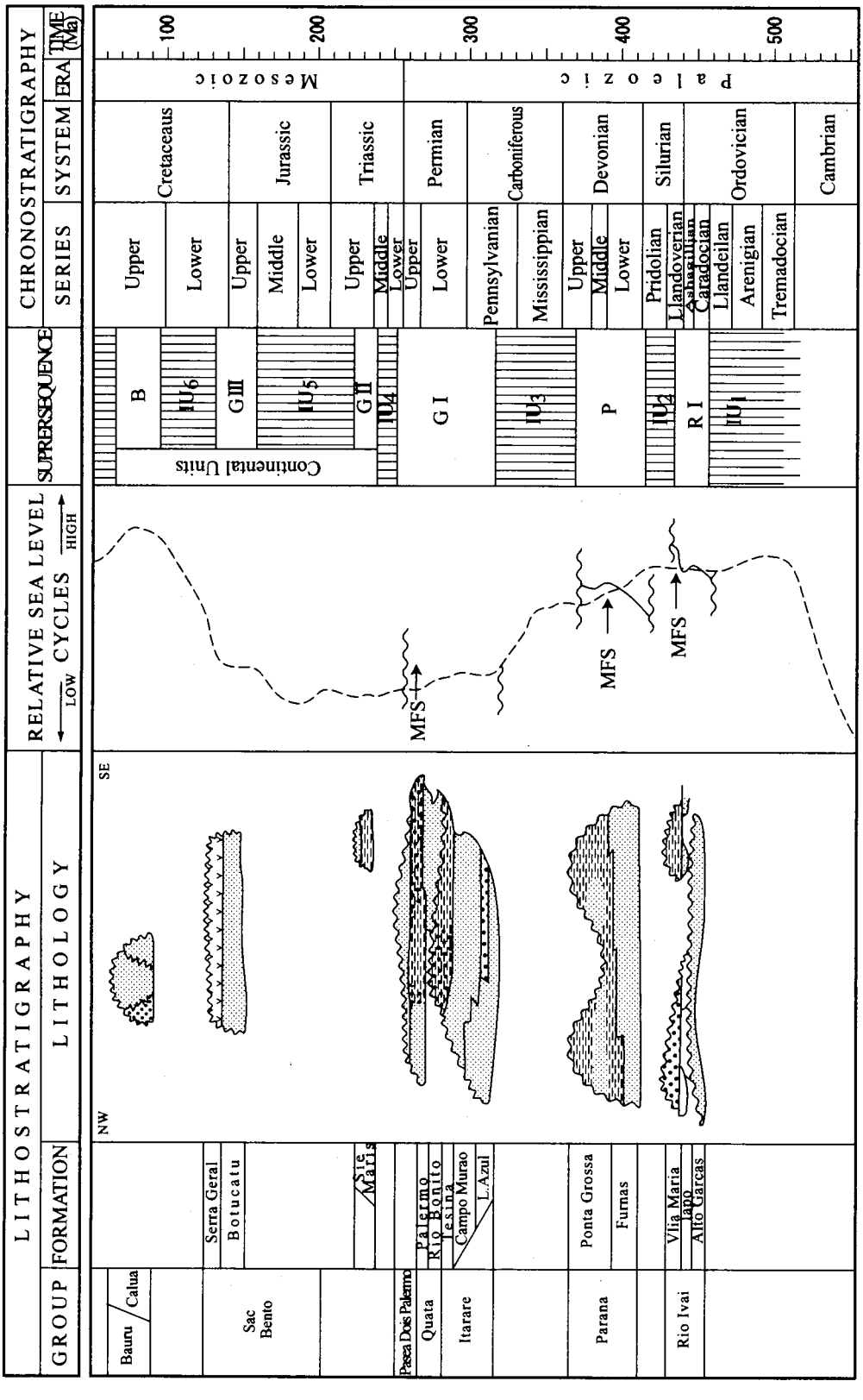

Fig. II-1-4-8 Sequence-stratigraphic chart for the Paraná basin

Relative sea level second order cycles derived from basin's statigraphic record and referred to Vail's(1977) first order eustatic cycles (dotted line). The correlation of supersequences with absolute geologic time is approximate. Time table after Cowie & Bassett(1989). IU-interregional unconformity. Lithostratigraphic names for the Upper Permian/Lower Triassic interval: (E.J.Milani et al., 1998)

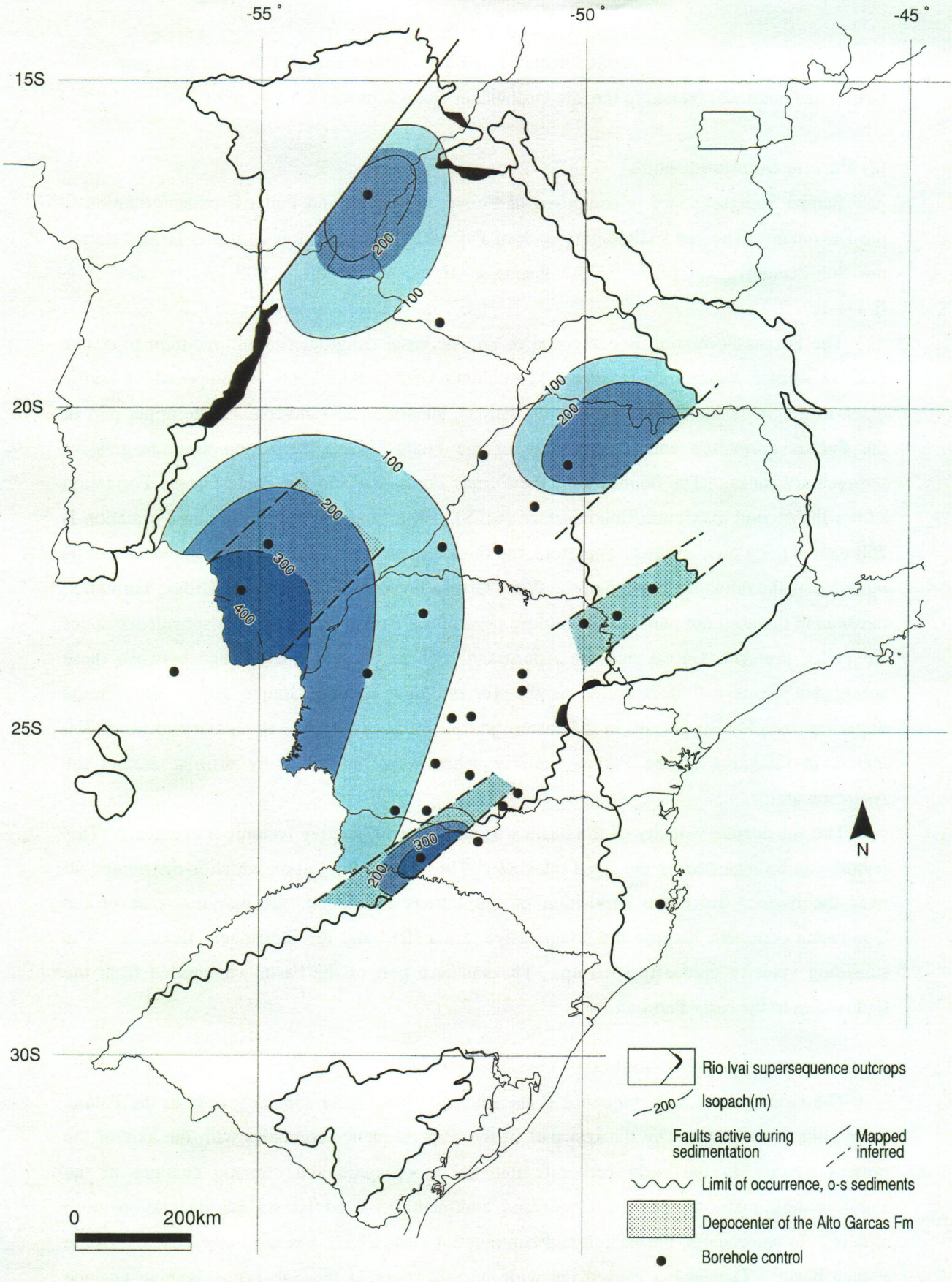

Fig. II-1-4-9 Isopach map of the Rio Ivai Sequence (E.J. Milani et al., 1998)

This extensional stress field formed synclise and intracratonic basin in the marginal part of the Gondwana continent related to the late Ordovician Ocloyic orogenic movement.

(2) Paraná Supersequence

Paraná Supersequence is composed of Furnas Formation and Ponta Grossa Formation in the Devonian. The last sedimentary rock of Paraná Supersequence was mostly eroded during the Sub-Pennsilvanian period. The thichness of the Formation is 900 meters thick (Fig. II-1-4-10).

The Furnas Formation is composed of arkosic basal conglomerite and medium to coarse grained whitish kaolinitic sandstone. The Ponta Grossa Formation is composed of neritic black to grayish shale (including organic matter), siltstone and sandstone. The upper part of the Furnas Formation and to the shale of the Ponta Grossa Formation are transgressive sedimentary rocks. The boundary of the Furnas Formation and the Ponta Grossa Formation shows the second maximum flood surface (MFS). The sandstone of the Frunas Formation is 250 meters thick on average. Therefore, the thickness change in Paraná Supersequence can be regarded as the thickness change of the Ponta Grossa Formation. The Ponta Grossa Formation thickens in the northern part and the middle arrea of the Paraná basin. These subsidence zones are called the Alto Garcas and the Apucarana. There is an upheaval zone between these subsidence zones and it is called as the Torres Lagos-Campo Grande arch. The Paraná Supersequence is also present in the eastern part of Paraguay. The sedimentary rocks of 850 meters in thickness of the Paraná Supersequence were confirmed by drilling around the Asuncion arch.

The subsidence velocity of the basin was slow due to inactive tectonic movement. This feature can be regarded by the fixed thickness of the Furnas Formation which is distributed all over the basin. Since the deposition of the Furnas Formation, the marginal part of the Gondwana continent became the compressive stress field and the lithosphere flexured. The subsiding velocity gradually sped up. The southern part of the basin was eroded from the Ordovician to the early Permian.

(3) Gondwana I Supersequence

The Gondwana I Supersequence is the thickest of the other supersequence in the Paraná basin (Fig. II-1-4-11). The thickest part of the Supersequence coincides with the axis of the present basin. In the early carboniferous, the topographic and climatic changes in the south-western marginal part of Gondwana continent involved lacuna (sedimentation stop) widely. In some parts, the lacuna had continued 45 Ma which was the longest lacuna in the Paraná basin. The lacuna caused the wide unconformity of the Sub-Pennsylvanian and the lack of Mississippian.

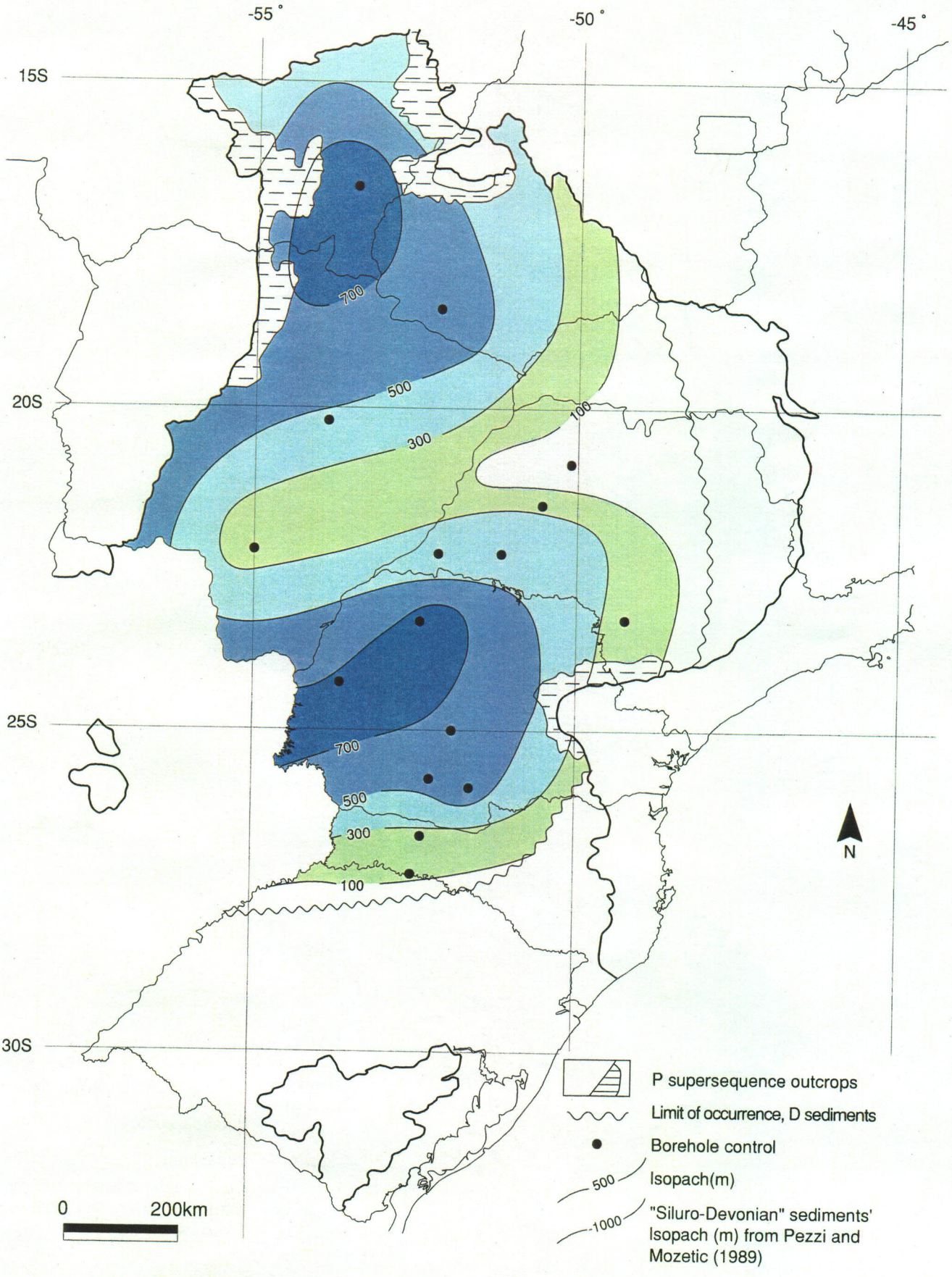

Fig. II-1-4-10 Isopach map of the Paraná supersequence (E.J. Milani et al., 1998)

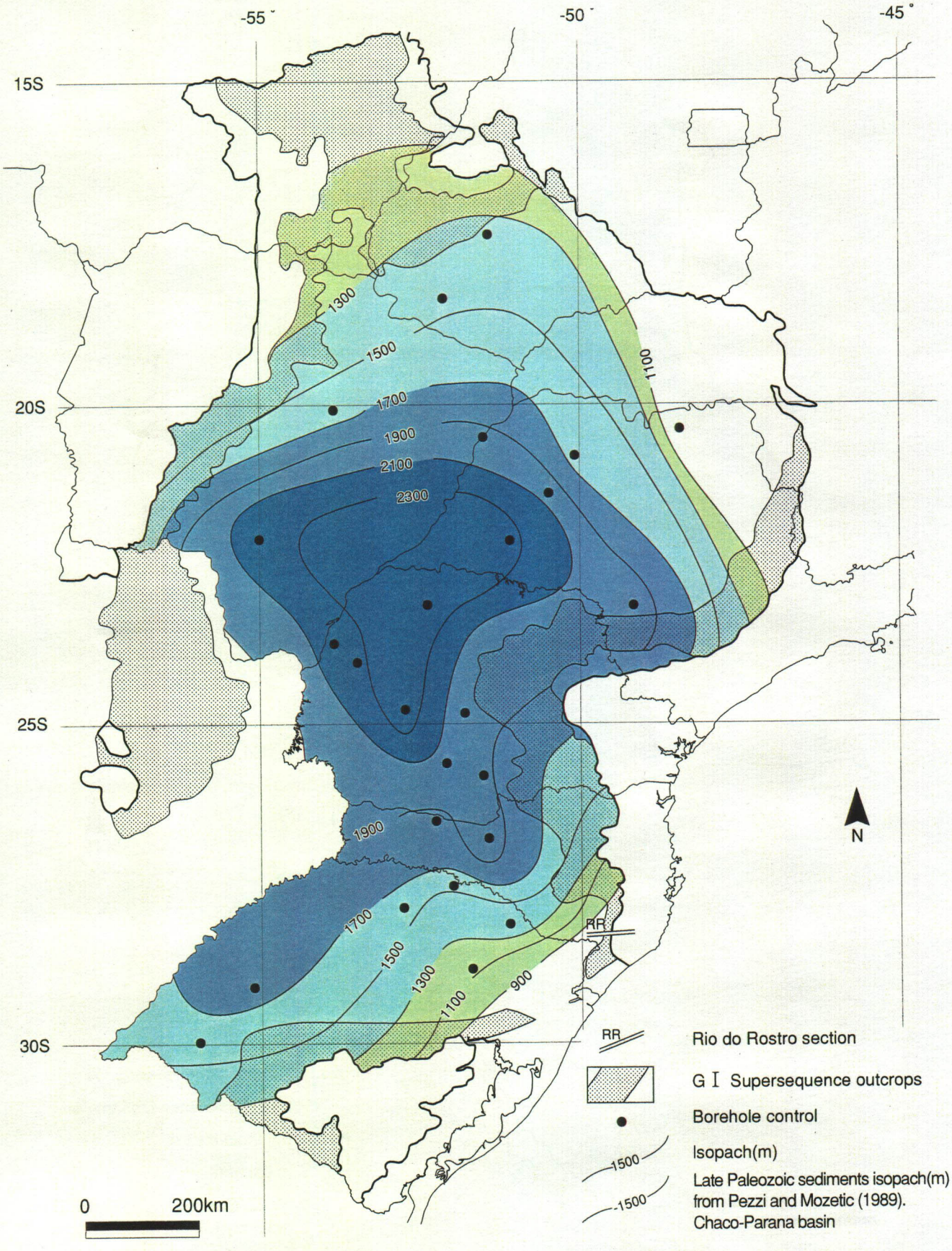

Fig. II-1-4-11 Isopach map of the Gondwana I supersequence (E.J. Milani et al., 1998)

A remarkable environmental change can be observed between the marine shale of the Ponta Grossa Formation in the Paraná Supersequence and the glacier sediments of the Itarare Formation in the Gondwana I Supersequence. Two reasons for this environmental change can be considered. One is the Hercynian orogenic movement which had continued approximately 50 Ma and successively the peneplanation. Another is denudation of glacier and resedimentation after the glacier epoch. In the late Carboniferous to Permian, a transgression occurred due to the melting of the glaciers and the rise in the sea surface. In this period, the Itarare Formation, Rio Bonito Formation and Palermo Formation were deposited. The upper part of Palermo Formation was deposited during the maximum flood surface (MFS). The cycle of transgression-regression finished to form the Red Rock Formation in the early Triassic. The Itarare Formation is mainly composed of diamictite and thick sandstone layers which are intercalated with diamictite. The Rio Bonito Formation is composed of coal (delta sediment), siltstone shale and sandstone. The Palermo Formation is composed of siltstone and sandstone.

The compressive stress field gradually increased in the south-western marginal part of Gondwana continent, and the Asuncion arch rose outside the western part of the basin. Finally, in the late Permian to the early Triassic, the basin was isolated from the ocean by the Asuncion arch. Since this period, the desertification and erosion continued for a long period within the continent. The Assitencia Formation overlies the Irati Formation and is composed of vitrinitic black shale, marl and limestone. These show rhythmical alterations with a thickness of approximately 10 centimeters. The Assitencia Formation includes evaporite layers of several tens centimeters in thickness in some limited shallow basins. The subsidence of the middle part of the basin lasted for a long period, however, the subsidence velocity gradually decreased in the late Permian to the early Triassic due to an extensional stress field.

(4) Gondwana II Supersequence

The Cape La Venrtana orogenic movement occurred in the southern margin of the Gondwana continent in the middle to late Triassic. The local upheaval and the lateral fault rock by the orogenic movement occurred along the lineaments of the basement. In the period, the extentional stress fields sometimes occurred in the south-western part of the Gondwana continent and they involved a graven. The Santa Maria Formation was deposited in a part of the Paraná basin in the middle to the late Triassic (Fig. II-1-4-12). The Santa Maria Formation is composed of fine to medium grained white sandstone and conglomeratio, and partly red shale, siltstone, calcrete and gypsum layers. These components are fluviatile-lacustrine deposits. The subsidence velocity was slow due to the Gondwana continent was stable.

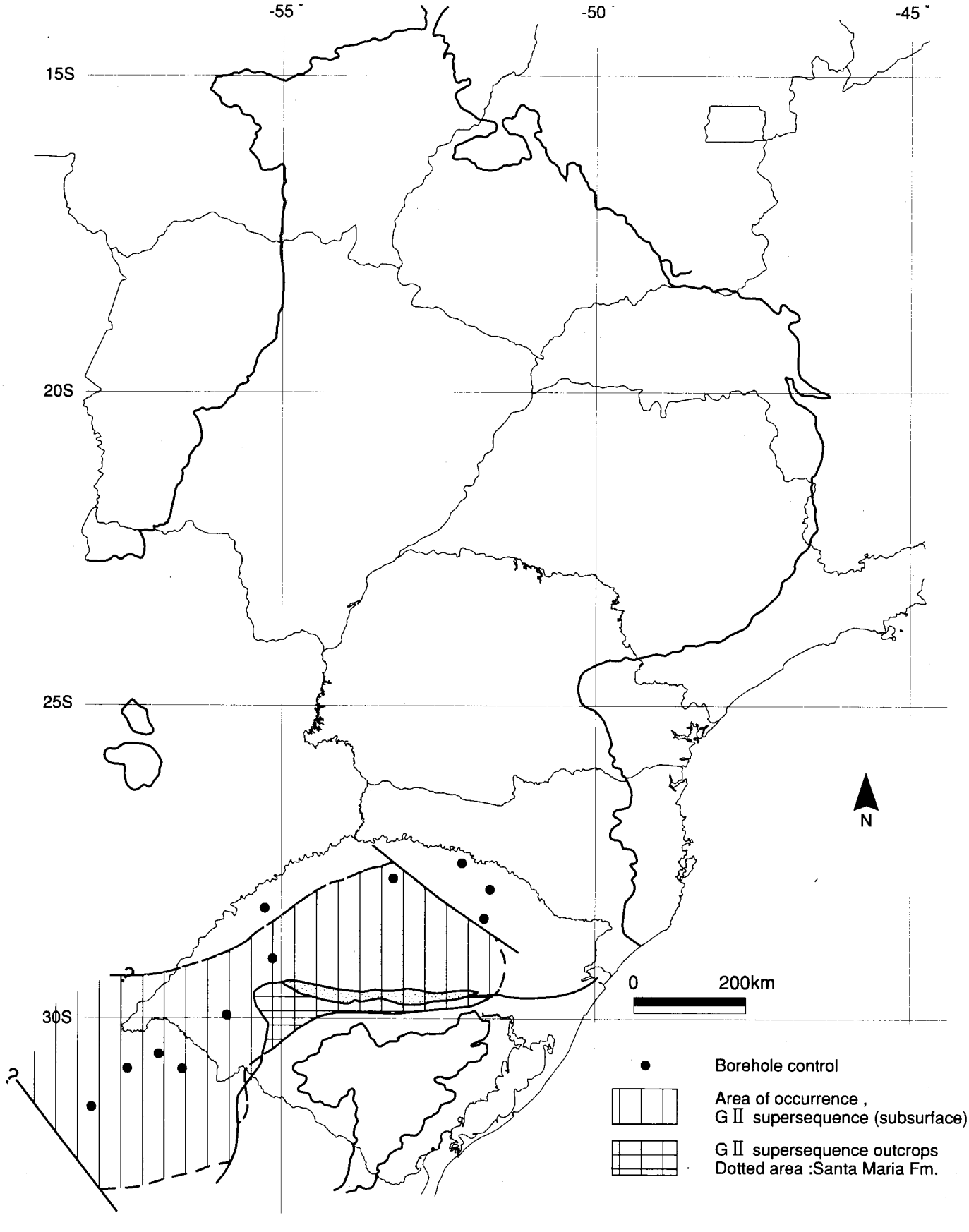

Fig. II-1-4-12 Occurrence of the Gondwana II supersequence (E.J. Milani et al., 1998)

(5) Gondwana III Supersequence

The lower part of the Gondwana III Supersequence is composed of fine to medium-grained quartzite and eolian sandstone which is called the Botocau Formation (Fig. II-1-4-13). Paraná flood basalt lava is distributed in the whole Paraná basin which covers or intercalate the Botocau Formation. The magma activity of the Paraná flood basalt formed huge volumes of lava and dykes and has a maximum thickness of 2,000 m under the maximum extentional stress field in the early Cretaceous. The subsidence velocity was the fastest due to the magma activity of Paraná flood basalt. Just after the subsidence, the development of the basin finished to form the deposition of the Baul Formation.

(6) Bauru Supersequence

In the middle to the late Cretaceous, the flexure pilling up of flood basalt lava involved the subsidence of the basin and the Bauru Supersequence is deposited. The Bauru Supersequence is composed of sandy conglomeratios including many kinds of gravel. The Bauru Supersequence is distributed in the central part to northern part of the Paraná basin (Fig. II-1-4-14). The history of the Paraná basin had finished by the end of the Bauru Supersequence.

1-4-4 Basement Structure Analyzed by Geophysical Data

The study of the earth's interior with the gravity data has been based on isostasy theory. M.C.L. Quintas (1995) discussed the structure of basement rocks of the Paraná basin using the isostasy model with gravity data and the thermodynamic model with oil-well drilling data.

(1) Origin of the Intracratonic Basin

The theory that the intracratonicic basin was formed by the subsidence movement of the basin caused by thermodynamic activity of the earth's interior is most popular recently (Bott, 1971; Sleep (1971); McKenzie et al. (1978)). Bott (1981) described that the active mechanism (plume rising) and passive mechanism (extentional stress) are two origins of the intracratonicic basin (Fig. II-1-4-15).

In the case of the active mechanism, (1) The lithosphere is flexured by the rising and heating of the plume. The distensible stress field develops on the ground surface to form normal faults. (2) The axis of the distensible stress field is eroded and the thickness of the lithosphere decreases. (3) The thinning part of the lithosphere subsides by cooling and the intracratonicic basin is formed

In the case of the passive mechanism, (1) The thickness of the lithosphere decreases due to the horizontal extentional stress field and asthenosphere rises. (2) Normal faults and graven is

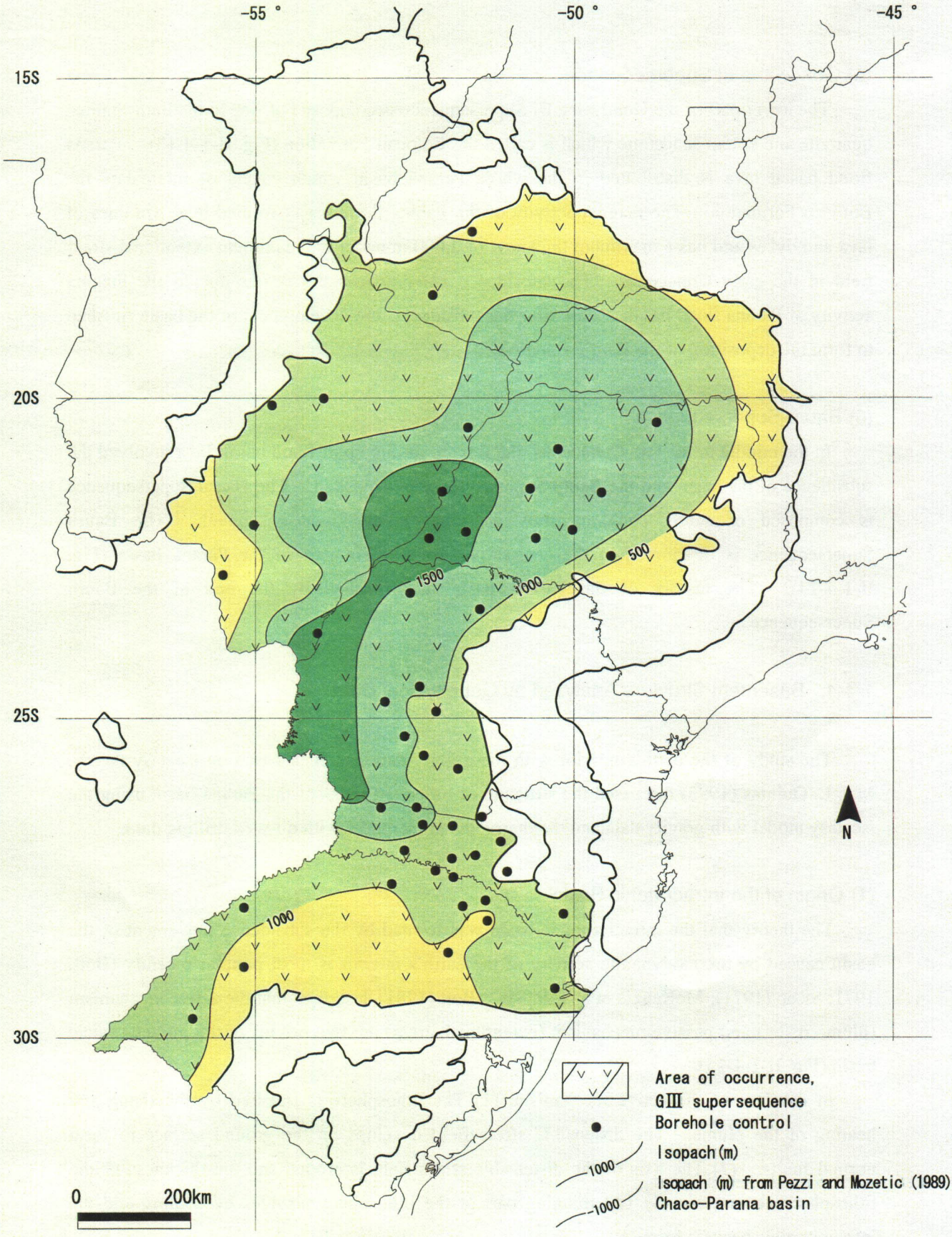

Fig. II-1-4-13 Isopach map of the Gondwana III supersequence sediments + volcanics (E.J. Milani et al., 1998)

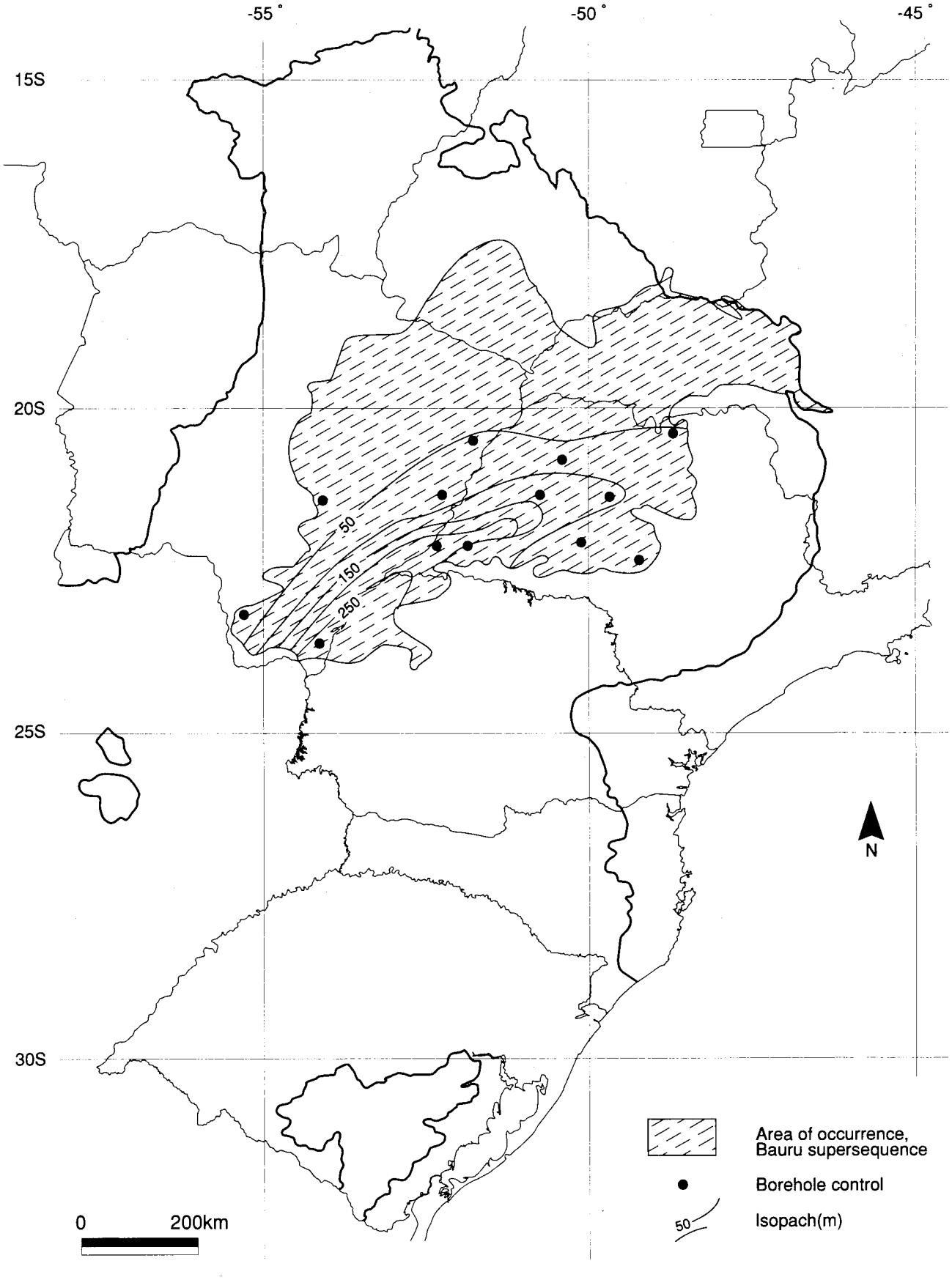

Fig. II-1-4-14 Isopach map of the Bauru supersequence (E.J. Milani et al., 1998)

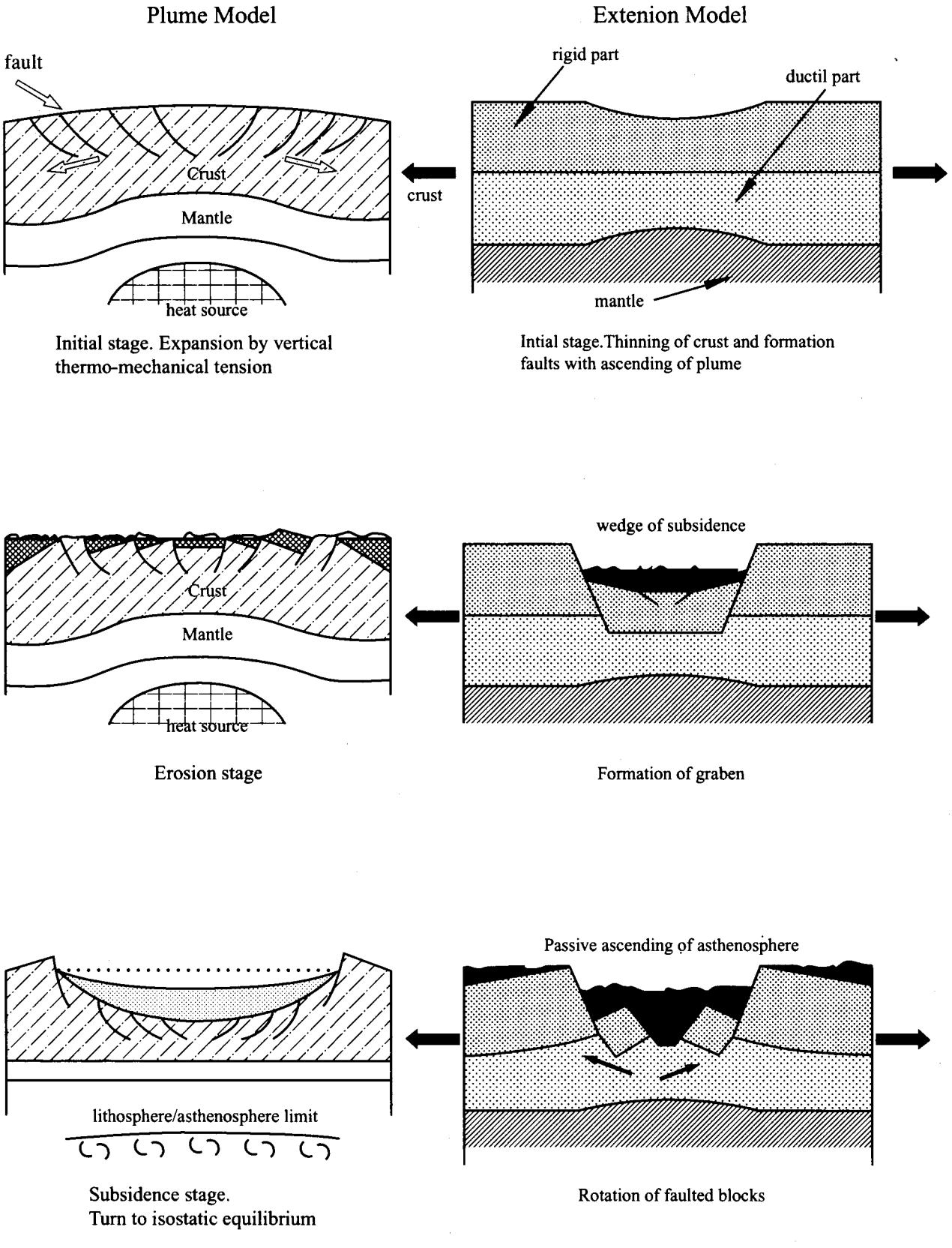

Fig. II-1-4-15 Genetic models of the intracratonic basin (Bott, 1981)

formed by downward flexure of the lithosphere. (3) The Asthenosphere rises and the lithosphere subsides under the extentional stress field.

There are several intracratonic basins in the world (Table II-1-4-1). These basins have several common points such as the beginning of sedimentation before the ruputure of Gondwana continent and the forming of rift before subsidence. These basins are presumed to be systematically formed by the origin of the earth's scale.

Table II-1-4-1 Intracratonic basin in the world

Basin	Locality	Thickness (m)	Initiation (Ma)	Duration (Ma)
Paraná	S.America	6,000 m	450 Ma	300 Ma
Illinois	N.America	6,000 m	510 Ma	300 Ma
Williston	N.America	3,700 m	500 Ma	310 Ma
Michigan	N.America	4,500 m	520 Ma	220 Ma
Parnaiba	S.America	4,000 m	500 Ma	300 Ma
Chad	Africa	develop	30 Ma	Develop

M.C.L. Quintas (1995)

(2) Data Analysis Method

Two individual methods were used for the data analysis. (1) Stress analysis using a thermodynamic model (β or ε : extension / attenuation factor). Ggeological data from 81 oil exploration drillings were used in this analysis. The McKenze (1978) model and Royden & Keen (1980) model, based on the theory of the extentional stress field, were used as the thermodynamic model. (2) Gravity data based on the isostasy model was analyzed. The data on the thickness of each layer of the Paraná basin was used. Besides this data, gravity data, seismological data and drilling data were used in this analysis.

a) Thermodynamic Model

When magma is generatiod within the asthenosphere, the continental lithoshere instantly (t = 0) shrinks β (Fig. II-1-4-16). When the magma penetratios to the lithosphere, the density of the lithosphere increases and at the moment the lithosphere subsides by isostasy. As a result, lifting occurred at the upper part of the lithosphere (crust) and the rift valley is formed. The initial subsidence of the rift Si becomes the sum of the subsidence by rigid movement (S_{rigid}) and the subsidence by ductile movement of the lithosphere (S_{ductil}). The initial subsidence Si is indicated by the following equation.

Model of Mckenzie(1978)

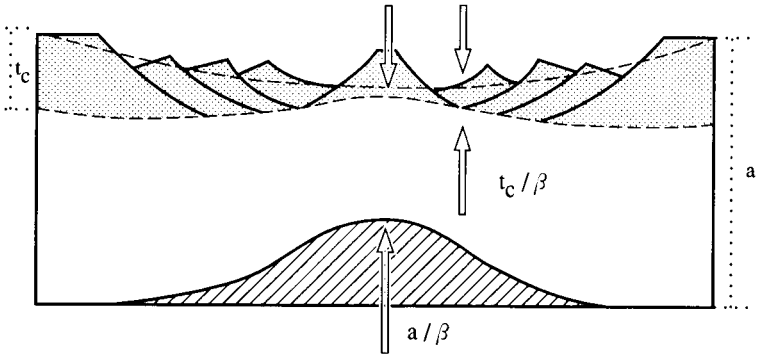

Model of Royden & Keen(1980)

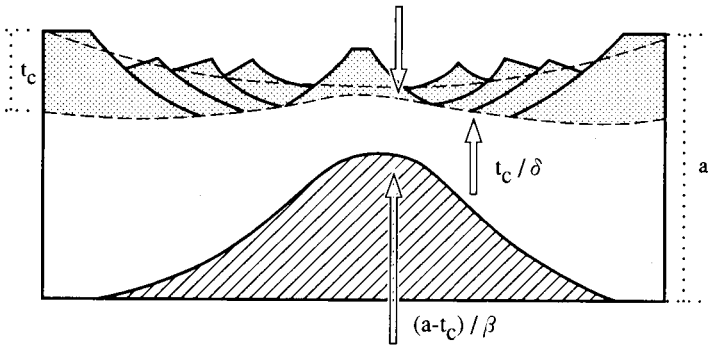

Fig. II-1-4-16 Thermomechanical model for formation of intracratonic basin

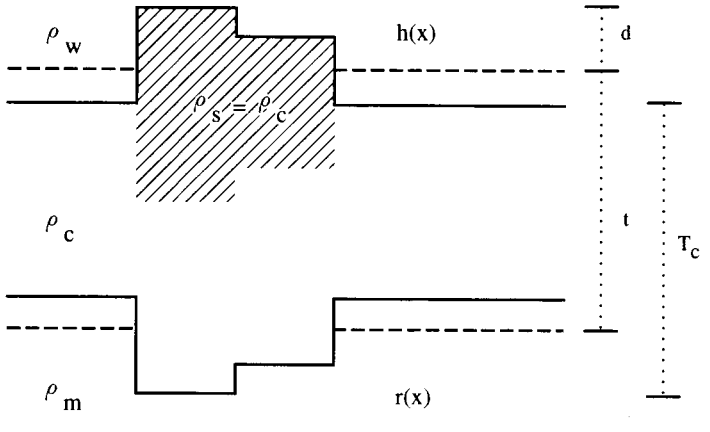

Fig. II-1-4-17 Isostatic model of Airy (Karner, 1982)

$$S_i = \frac{[(\rho_m - \rho_c)t_c(1-\frac{t_c \alpha T_m}{2a}) - \frac{a\alpha T_m \rho_m}{2}](1-\frac{1}{\beta})}{[\rho_m(1-\alpha T_m)-\rho_w]} \quad (5)$$

T_c = initial thickness of continental lithosphere
α = coefficient of thermal expansion
ρ_m = density of mantle
ρ_w = density of water
a = thickness of lithosphere
T_m = temperature of lithosphere basement
ρ_c = density of lithosphere
β = attenuation ratio

After initial subsidence of the basin, the lithosphere gradually refrigerates and attenuates and thermally subsides (flexural subsidence). This thermal subsidence St can be calculated by using the thermal conductivity equation. The total subsidence S total becomes the sum of the initial subsidence Si and thermal subsidence St.

$$S_t = e(0) - e(t) \quad (6)$$

$$e(t) = E_o(\frac{\beta}{\pi}\sin\frac{\pi}{\beta})\exp^{-\frac{t}{\tau}} \quad E_o = \frac{(4at_m \rho_m \alpha)}{\pi^2(\rho_m - \rho_w)} \quad (7)$$

$$S_{total} = S_i + S_t \quad (8)$$

The above is the Mckenze model (1978). This model is based on the premise of instant attenuation of the lithosphere (t is less than 20 Ma), however, refrigeration of magma is considered to continue more than 50 Ma. In this case, computational error of the subsidence is generatiod. Royden & Keen (1980) estimated that the thermal subsidence of magma by cooling became smaller than that of McKenze model. They divided the lithosphere's attenuation into the upper part δ and lower part β and calculated the attenuation ratio and the total subsidence (Fig. II-1-4-16).

$$\varepsilon = \frac{a}{\frac{t_c}{\delta} + (a - t_c)\beta} \quad (9)$$

b) Backstripping Method

The Backstripping method is the adequate method to calculate the thickness of the sediments through the history of the basin. The method is to release the target sedimentary layer from the consolidation pressure by stripping the layers younger than the target layer. The layer which is released from consolidation pressure rises to the initial horizon. The subsiding depth of the basement by the sediments can be obtained by calculating the thickness of the sedimentary layer in each period. The actual depth of basement Y can be calculated, compensating the effect of load of the sediments by the following equation which was proposed by Sclater and Christie (1980).

$$Y = S\left(\frac{\rho_m - \overline{\rho_s}}{\rho_m - \rho_w}\right) \qquad (10)$$

ρ_w = density of water,
ρ_s = average density of sediment
S = measured total thickness of sediments,
ρ_m = density of mantle

c) Isostasy Correction

Although the ordinary Bouguer anomaly reduction is effective to reduce the influence of local topography, it is not enough to reduce the influence of large scale topography. For example, in case of a small mountain with 10 kilometers extension, the lithosphere can support the mountain without deformation. But, in the case of a mountain system with 1,000 kilometers extension, the lithosphere bends downward and isostasy correction becomes necessary.

The weight of the lithosphere keeps in equilibrium by flexure of the rigid lithosphere on the ductile asthenosphere according to Barrel (1914a). Because the rocks of the lithosphere are lighter than those of the asthenosphere, the Mass of the big mountain system is compensated by the depth of low density roots. Because the existence of roots are not reflected in the Bouguer anomaly correction, the Bouguer anomaly in the big mountain system indicates a large minus value. This minus anomaly is called the isostasy anomaly, which can be corrected by isostasy correction (Fig. II-1-4-17).

The Fourier transformation GT (k) of the gravity anomaly which is caused by isostasy is shown in the following equation by Karner (1982) and Karner & Watt (1982).

$$G_T(k) = 2\pi\gamma\,\Delta\rho_1\,H(k)\exp^{-kd}\left[1-\frac{\Delta\rho_2\,R(k)\exp^{-kt}}{\Delta\rho_1\,H(k)}\right] \quad (11)$$

$H(k)$ = Fourier transFormation of gravity $h(x)$ on the topographic surface
$R(k)$ =Fourier transFormation of gravity $R(x)$ on the topographic root
$\Delta\rho_1$ = density difference of the topographic surface
$\Delta\rho_2$ = density difference of root
d = average height,
t = distance between average topographic surface and opographic root,
γ = gravity constant,
k = wave number ($2\pi/\lambda$),
λ = wave length

(3) Data

The drilling data for petroleum prospecting of the DEPEX-PETROBORAS Corporation and the gravity data of the Research Institutes of IAG/USP, IBGE, ON and CPRM & UFPR were used. PETROBORAS Corporation and PETEROPAULI Corporation carried out 73 drillings and 33 drillings respectively until 1985. M.C.L. Quintas (1995) used 81 of these drilling data. The drilling locations are shown in Fig. II-1-4-18, Table II-1-4-2). The La Costa & Romberg G gravimeter was used for gravitation measurement. The Bouguer anomaly was corrected inrnational Gravimetric Formula (1967) and average density 2,670 kg/m^3. Topographic reduction was not carried out because of the flat topography of the Paraná region. Thermal conductivity (K), porosity (ϕ) and decreasing ratio (c) are used referring to The IPT Report.

(4) Results of Analysis

a) Subsidence Curve by Backstripping Method

The depth of the basement was calculated using equation (10), classifying rock facies of sediments into five types (sandstone, crystalline schist, limestone, siltstone and basalt) and fixing each porosity (ϕ) and decreasing ratio (c) (Fig. II-1-4-19, Table II-1-4-3).

Presuming the total formative period of the basin to be 440 Ma and total thickness of the sediments to be 6,000 meters as the preconditions, the average subsiding ratio of the basement becomes 13.6 m/Ma. The sedimentation periods are 414-410 Ma, 367-296 Ma, 248-238 Ma, 213-188 Ma, 65-0 Ma, totally 184 Ma by subsidence curve and geological data. Presuming the 10 percent erosion ratio of sediments, 600 meters of sediments are eroded in 184 Ma and a 3.3 m/Ma of erosion ratio is obtained. Therefore, the average subsiding ratio of the basement is 16.9 m/Ma as the erosion correction.

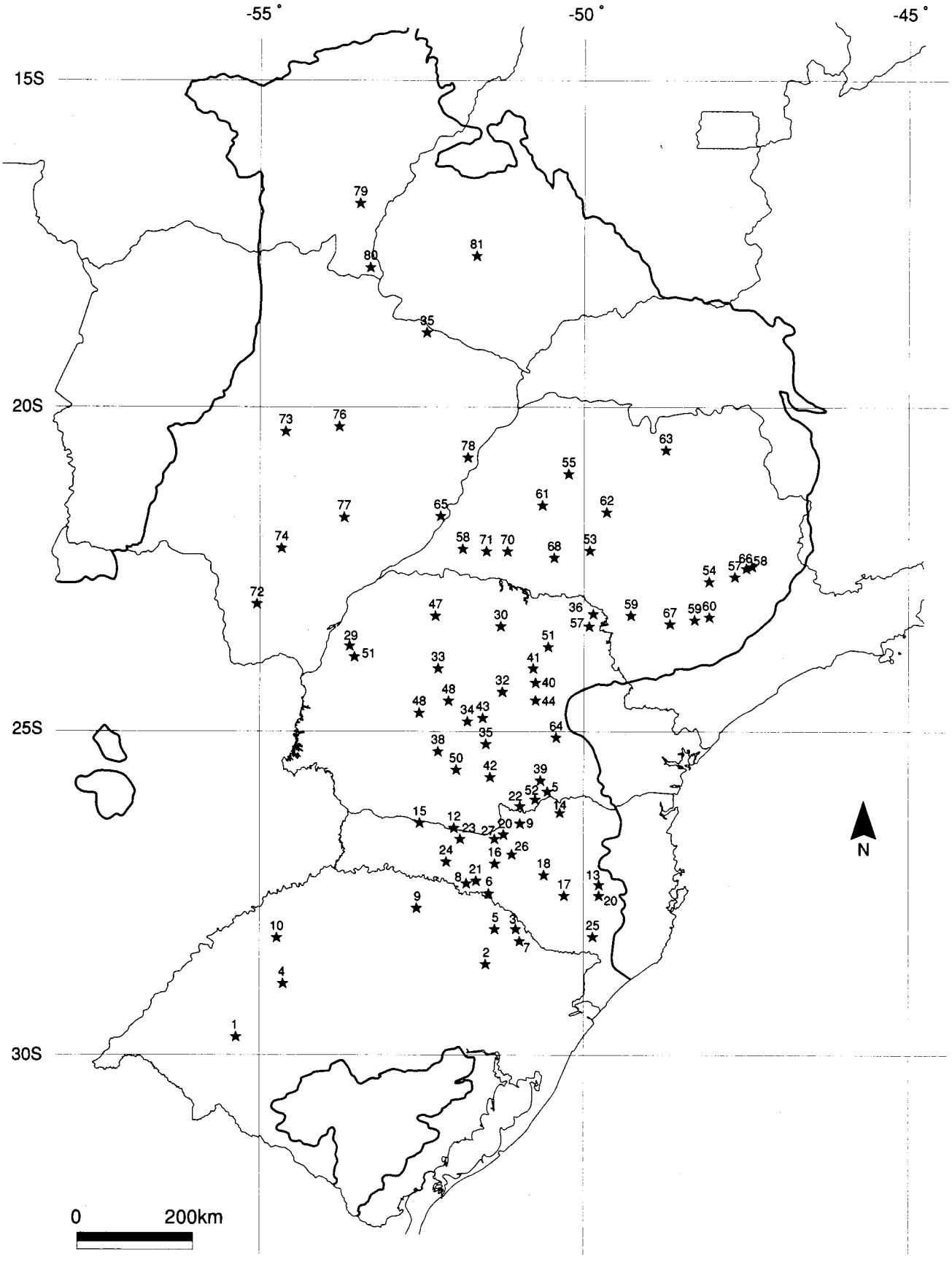

Fig. II-1-4-18 Locations of drilling holes used by M.C.L. Quintas (1995)

Table II-1-4-2 Locations of drilling holes (M.C.L. Quintas, 1995)

Name	City	#	Prillory	LATITUDE (°)	LONGI TUDE (°)
Alegrete	Alegrete	1	2-AL-1	-29,80216	-55,76664
Atanásio	Nova Prata	2	2-AO-1	-28,70143	-51,66456
Esmeralda	Esmeralda	3	1-ES-1	-28,17864	-51,17861
Itacurubi	Santiago	4	2-IT-1	-29,01666	-54,99165
Lagoa Vermelha	Lagoa Vermelha	5	2-LV-1	-28,16354	-51,50276
Machadinho	Machadinho	6	1-MA-1	-27,58679	-51,66314
Muitos Capões	Vacaria	7	1-MC-1	-28,35206	-51,11268
Marcelino Ramos	Marcelino Ramos	8	2-MR-1	-27,50741	-51,90275
Ronda Alta	Ronda Alta	9	2-RD-1	-27,83906	-52,76718
Rio Ijuf	Rio Ijuf	10	2-RI-1	-28,29998	-55,04998
Torres	Torres	11	2-TO-1	-29,32604	-49,79139
Abelardo Luz	Abelardo Luz	12	2-AL-1	-26,45031	-52,18131
Barra Nova	Barra Nova	13	1-BN-1	-27,51242	-49,75526
Canoinhas	Canoinhas	14	2-CN-1	-26,26890	-50,51927
Galvão	GAlvão	15	1-GO-1	-26,38268	-52,70943
Herval Velho	Herval Velho	16	1-HV-1	-27,21578	-51,46365
Lajes	Lajes	17	2-LA-1	-27,62966	-50,39526
Marambas	Curitibanos	18	1-MB-1	-27,32490	-50,73741
Matos Costa	Matos Costa	19	1-MC-2	-26,53240	-51,16127
Petrolândia	Petrolândia	20	1-PA-1	-27,59428	-49,73251
Piratuba	Piratuba	21	2-PI-1	-27,42579	-51,78401
Porto União	Porto União	22	2-PU-1	-26,26654	-51,05752
Rio Chapecó	Ponte Serrada	23	1-RCH-1	-26,65456	-52,04381
Seara	Seara	24	1-SE-1	-27,14331	-52,29831
São Joaquim	São Joaquim	25	1-SJQ-1	-28,27128	-49,91664
Tangará	Tangará	26	2-TG-1	-27,09529	-51,24427
Três Pinheiros	Ãgua Doce	27	1-TP-3	-26,78443	-51,47568
Taquara Verde	Caçador	28	2-TV-1	-26,74703	-51,31477
Altônia	Altônia	29	2-AN-1	-23,85456	-53,80681
Apucarana	Apucarana	30	2-AP-1	-23,49690	-51,42150
Alto Piquiri	Alto Piquiri	31	2-AP1-1	-24,00000	-53,71667
Cândido de Abreu	Cândido de Abreu	32	1-CA-1	-24,52191	-51,38116
Campo Mourão	Campo Mourão	33	2-CM-1	-24,14190	-52,41140
Chapéu do Sol	Pitanga	34	2-CS-1	-24,96406	-51,96473
Guarapuava	Guarapuava	35	2-GP-1	-25,30543	-51,65681
Jacarezinho	Jacarezinho	36	1-J-1	-23,22889	-49,95227
Joaquim Távora	Joaquim Távora	37	1-JT-1	-23,46803	-49,94966
Laranjeiras do Sul	Laranjeiras do Sul	38	2-LS-1	-25,40080	-52,41102
Mallet	Mallet	39	1-M-1	-25,86915	-50,78576
Monjolinho	Monjolinho	40	1-MO-1	-24,37329	-50,87615
Ortigueira	Ortigueira	41	2-O-1	-24,18103	-50,88900

Name	City	#	Prillory	LATITUDE (°)	LONGI TUDE (°)
Pinhão	Pinhão	42	1-PH-1	-25,82482	-51,59075
Pitanga	Pitanga	43	1-PT-1	-24,93268	-51,75518
Reserva	Reserva	44	1-R-1	-24,62266	-50,88491
Rio Claro do Sul	Rio Claro do Sul	45	1-RC-1	-26,01330	-50,70451
Rio do Canto	Alto Paraná	46	1-RCA-1	-24,82831	-52,70100
Rio Ivaí	São Caetano do Ivaí	47	2-RI-1	-23,33131	-52,45518
Roncador	Roncador	48	1-RO-1	-24,61206	-52,24856
Rio Piquiri	Palmital	49	2-RP-1	-24,82831	-52,70131
Rio Segredo	Mangueirinha	50	1-RS-1	-25,70581	-52,11668
PRS. Jerônimo da Serra	PRS. Jerônimo da Serra	51	1-SJ-1	-23,78260	-50,66413
União da Vitória	União da Vitória	52	2-UV-1	-26,17903	-50,92866
Amadeu Amaral	Marília	53	2-AA-1	-22,30243	-50,04193
Anhembi	Piracicaba	54	2-AB-1	-22,77853	-48,18202
Araçatuba	Araçatuba	55	2-AR-1	-21,12818	-50,37406
Assistência	Assistência	56	2-AS-1	-22,51690	-47,58190
Artemis	Artemis	57	1-AT-1	-22,66778	-47,80491
Cuiabá Paulista	Cuiabá Paulista	58	1-CB-1	-22,30331	-52,03931
Carlota Prenz	Angatuba	59	1-CP-1	-23,37153	-48,38751
Guarei	Guarei	60	2-GU-3	-23,34254	-48,20576
Lagoa Azul	Osvaldo Cruz	61	2-LA-1	-21,65418	-50,79318
Lins	Lins	62	2-LI-1	-21,69227	-49,75616
Olímpia	Olímpia	63	2-OL-1	-20,68754	-48,92776
Piratininga	Piratininga	64	1-PA-1	-25,17368	49,11356
Presidente Epitácio	Presidente Epitácio	65	2-PE-1	-21,75842	-52,10189
Piracicaba	Fazenda Pitanga	66	1-PG-1	-22,54449	-47,64022
Paranapanema	Paranapanema	67	2-PN-1	-23,45281	-48,77431
Paraguaçu Paulista	Paraguaçu Paulista	68	2-PP-1	-22,41828	-50,60464
Sarutaia	Sarutaia	69	1-SA-1	-23,28206	-49,42643
Taciba	Taciba	70	2-TB-1	-22,33381	-51,34668
Tarabaí	Tarabaí	71	1-TI-1	-22,5331	-51,67318
Amambai	Amambai	72	2-AM-1	-23,10990	-55,23664
Campo Grande	Campo Grande	73	2-CG-1	-20,48579	-54,71914
Dourados	Dourados	74	2-DO-1	-22,26803	-54,81275
Rio Aporé	Cassilândia	75	2-RA-1	-18,83568	-52,36043
Ribas do Rio Pardo	Ribas do Rio Pardo	76	2-RP-1	-20,42079	-53,87242
São Domingos	São Domingos	77	2-SD-1	-21,82778	-53,81565
Três Lagoas	Três Lagoas	78	2-TL-1	-20,87916	-51,75000
Alto do Garças	Alto do Garças	79	1-AG-1	-16,96066	-53,52491
Taquari	Alto Araguaia	80	2-TQ-1	-17,88166	-53,27465
Jataí	Jataí	81	2-JA-1	-17,80656	-51,78718

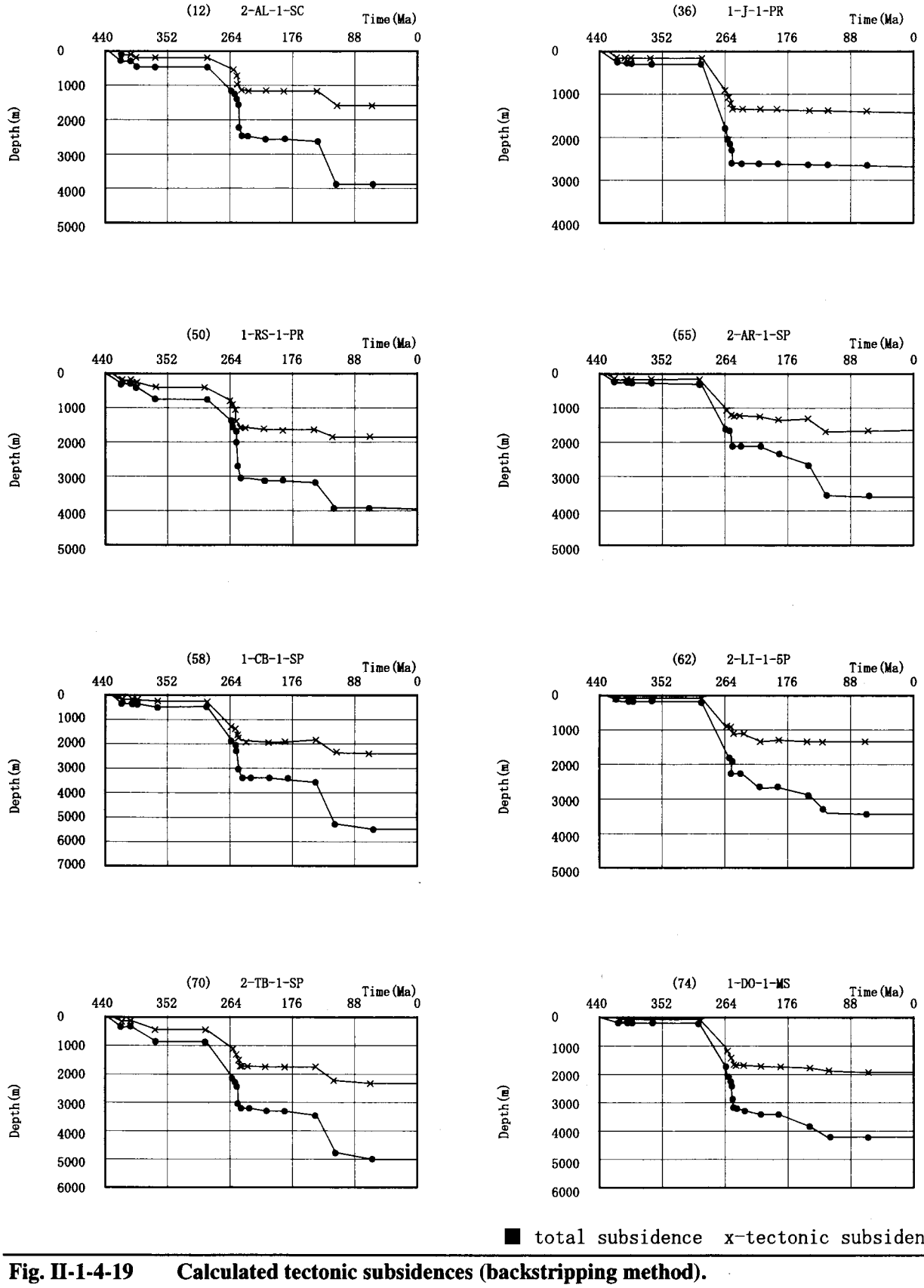

Fig. II-1-4-19 Calculated tectonic subsidences (backstripping method).
Drilling 12, 36, 50, 55, 58, 82, 70 e 74(M. C. L. Quintas 1995)

Table II-1-4-3 Basic Parameters used in thermomechanic model (M.C.L. Quintas, 1995)

parameter	value
Density of water	1.03 g/cm^3
Density of crust	2.80 g/cm^3
Density of mantle	3.33 g/cm^3
average density of lithosphere	2.8 g/cm^3
Temperature on the base of lithosphere	1.350 °C
Thermal diffusion of lithosphere	8.0 10^{-3} cm^2 s^{-1}
Average thermal conductivity of lithosphere	7.5 10^{-3} cat cm^{-1} $°C^{-1}$ s^{-1}
Thermal conductivity of water	1.35 10^{-3} cat cm^{-1} $°C^{-1}$ s^{-1}

Table II-1-4-4 Ratios of tectonic subsidence and total subsidence with the time with the time. The values in the parenthesis cerrespond to the averages for the time (M. C. L. Quintas, 1995).

Formations or Groups	$S_{tectonic}$ / time		S_{total} / time	
Grupo Rio Ivai	7		13	
Furnas	13		19	
Ponta Grossa	6		14	
Itararé	14		26	
Rio Bonito	17		39	
Palermo	30	(49)	71	(111)
Irati	33		58	
Teresina	42		178	
Rio do Rasto	92		137	
Pirambóia	3		6	
Botucatu	1		3	
Serra Geral	5		26	
Bauru	1		2	

Remarkable subsidence is observed in the period from the Palermo Formation to the Rio do Rast Formation (248-238 Ma). During this period, the structural subsiding and total subsiding ratios are 49 m/Ma and 111 m/Ma, respectively. This marked subsidence (sedimentation) is a common phenomenon in the rift basin which occurred worldwide after the Hercynian orogenic movement in the Permian to Triassic. In the case of Serra Geral Formation (Paraná flood basalt: early Cretaceous), the structural subsidence (5 m/Ma) is approximately 20 % of total subsidence (26 m/Ma) and is lower than those of other sedimentary rocks. The reason is considered to be that the load of the Paraná flood basalt being high density markedly affected the total subsiding ratio.

b) Attenuation Ratio by Thermodynamic Model (ε)

The attenuation ratios of the upper part β, the lower part δ of the lithosphere and the attenuation ratio ε of the whole lithosphere were obtained comparing to the structural subsiding curves and theoretical subsiding curves that were obtained by using the thermodynamic model and the Backstripping method, respectively. The basic parameters that were used in the thermodynamic model are shown in Table II-1-4-4.

Three activities are presumed by the subsiding curve. Those are: the first distensible period of activity (unconformity forming period): before the sedimentation of the Silurian to Devonian (before 440 Ma), the second distensible period of activity: before the sedimentation of the upper Carboniferous (before 296 Ma), the third expanding period of activity: before the eruption of the flood basalt of the Jurassic to Cretaceous (before 144 Ma). The attenuation ratio (ε) was calculated based on the crust thickness a = 45km by seismic data (by D.E. James et al., 1994) and the lithosphere thickness tc=150 km. M.C.L. Quintas (1995) confirmed that the thermodynamic model by Royden and Keen (1980) was more accuratio than the model by McKenze (1978) and used the former model.

The first distensible activity: ε is 1.01 to 1.32 (Fig. II-1-4-20). The high ε zone is observed in the western part to north-western part of Paraná Province near the eastern border of Paraguay in the NE – SW direction. This suggests that the western part to north-western part of Paraná Province was the thinner part of the lithosphere during this period in the NE – SW direction. The corresponding expanding stress field is presumed in the NW –SE direction. Furthermore, the high ε zone corresponds to the area where a large amount of sills and dykes intrude (Fig. II-1-4-21).

The high ε zone (approximately 1.16) is also recognized along W52° meridian in Mato Grosso do Sul extending in the direction of N-S. These results coincide with the results of Fig. II-1-4-9, Fig. II-1-4-10). By these facts, the sedimentation of the Rio Ivai Supersequence and Paraná Supersequence is assumed to begin in this part after the first distensible period of activity.